Statics and Fast Dynamics of Nanomagnets with Vortex Structure

R. Höllinger*, A. Killinger, U. Krey
Inst. für Physik II, Universität Regensburg, 93040 Regensburg, Germany

v1: April 23, 2002; v3: Nov. 11, 2002, accepted by JMMM

Abstract

Within the framework of the Landau-Lifshitz-Gilbert equation, using permalloy parameters, we study the statics and dynamics of flat circular magnetic nano-structures with an in-plane magnetic vortex configuration, putting particular emphasis on the *vorticity* of the magnetic state and on the (perpendicular) *polarisation* of the vortex center, which may be shifted with respect to the center of the circle. These binary degrees of freedom can in principle be used to manipulate *two independent bits* of information.

Studying switching processes induced by in-plane and out-of plane field pulses we find that it is possible to switch the vorticity of the magnetic dot on a time scale of 40 ps in strong enough and short enough perpendicular external field pulses ($B_z^{\rm ext} \approx 0.5$ T, duration ≈ 40 ps). But for realistically small values of the Gilbert damping, only the *vorticity* can be switched this fast, and it turns out that it is better to dismiss the center of the circle totally, concentrating on flat 'nano-rings' with an inner radius R_1 and an outer radius R_2. On these 'nano-rings' the vortex state is more stable, and with respect to the switching of the vorticity these structures have similar properties as circular dots.

PACS numbers/keywords:
75.75.+a Magnetic properties of nanostructures; 75.40.MG Numerical simulation studies; 75.40 Gb Dynamic properties
85.70-d Magnetoelectronics

*Corresponding author, e-mail rainer.hoellinger@physik.uni-regensburg.de

1 Introduction

Recently there is a strong interest in using small magnetic structures as storage elements and for fast magnetoelectronic computation (MRAMs, [1]). R. Cowburn, [2], has studied experimentally and by simulation arrays of flat magnetic structures with circular or square individual geometries, and M. Schneider *et al.*, [3], have considered more general geometries of the dots. The present state of the art concerning the static behaviour of magnetic nano-dots and their arrays is contained in the very recent papers of Ross *et al.*, [4], Metlov and Guslienko, [5], and Guslienko *et al.*, [6, 7]. Concerning the dynamics we explicitly mention the even more recent papers of Gerrits *et al.*, [8], and Novosad *et al.*, [9], and the references therein.

If for a given thickness the radius R of the flat dot is smaller than a critical value R_c (see below), then the dot is in an in-plane single-domain state, whereas for $R > R_c$, the dot is magnetically in a *vortex state*, see [2].

Below, for flat dots, i.e. for small values of their *aspect ratio* $a := (t_h/R) \ll 1$, where t_h denotes the *thickness* of the dot, at first (for given R) the critical thickness t_c is calculated for structures with permalloy material parameters, and a considerable stability range for the magnetic vortex state is obtained even in rather tiny nano-structures. By application of a sufficiently small in-plane static magnetic field the magnetic state of the dot does not change topologically, i.e. the vortex center shifts, however the vorticity is still well-defined, and also the central direction of the magnetization (so-called "central polarisation" $\pm$) is unchanged. At the vortex center and in the region nearby, the magnetization (which must be constant in magnitude) is out-of-plane, whereas far from the center it is of course in-plane.

Therefore the magnetic vortex state of the dot has a fourfold topological degeneracy, since in principle one can measure (and *flip*) independently both the *vorticity* (r/l) of the state and the *central polarisation* $(+/-)$ of the vortex; *i.e. one has two bits per dot for a 'vortex-state dot', instead of only one bit for 'single-domain dots'.*

At present, the *vorticity* of the dot can be measured e.g. by electron microscopy in the Lorentz mode while the *central polarisation* can be measured e.g. by magnetic force microscopy, [10]: Of course, for the applications one should find more convenient methods; but this task is

not considered here. In any case, the possibility of storing and switching two independent bits of information instead of only one, and the fact that one does not rely on the extremely small single-domain dots, gives a strong additional motivation to study the statics and dynamics of circular dots in the vortex state very thoroughly.

In the following chapter 2 we introduce the basic micromagnetic tools for such a study, the Landau-Lifshitz free energy functional and the dynamical Landau-Lifshitz-Gilbert equation, [11]. In chapter 3, the behaviour of flat circular dots under static external magnetic *in-plane* fields is considered, with particular emphasis on the transitions between the vortex state and the in-plane single-domain state, whereas in the next chapter 4 we consider the dynamics, both for in-plane fields and perpendicular field-pulses. The switching-dynamics is exemplified by some kind of "movie representation" for typical cases, which show that the time scale, $\tau \sim 40$ ps, for the precessional switching of the vorticity by strong perpendicular field pulses, $H_z^{\text{ext}} \sim 5000$ Oe over this duration, is extremely short, whereas the polarisation of the vortex core cannot be reliably switched at all on these time scales, see below. Therefore at the end, it is natural to skip the vortex center totally by considering in chapter 5 flat *nano-rings*, i.e. circular structures with an inner radius R_1 and an outer radius R_2, which are both small, i.e. of the order of 50 to 150 nm, but large compared to the thickness t_h. We find that in this case the stability of the information is significantly improved and the switching dynamics is as fast as before.

2 Basic equations

Let us write the magnetic polarisation $\vec{J}(\vec{r},t)$ as $\vec{J}(\vec{r},t) = J_s \cdot \vec{\alpha}(\vec{r},t)$, where $J_s = |\vec{J}|$ is the constant *magnitude* and $\vec{\alpha}(\vec{r},t)$ the position- and time-dependent *direction* of the magnetic polarisation. We neglect in the following the small (in-plane) uniaxial magnetic anisotropy of Py, taking only the exchange interaction, the magnetic dipole-dipole interaction, and the Zeeman interaction (i.e. the interaction with the external magnetic field) into account. As a consequence, the Free Energy of the magnetic system K considered is obtained by minimization

of the following "Landau-Lifshitz functional", see e.g. [12, 13]:

$$F_{LL} := \int\limits_{V(K)} \mathrm{d}V \cdot \left\{ A \sum_{i=1}^{3} (\frac{\partial \vec{\alpha}}{\partial x_i})^2 - J_s \cdot (\frac{1}{2}\, \vec{H}^{\mathrm{Dip}} \cdot \vec{\alpha} + \vec{H}^{\mathrm{ext}} \cdot \vec{\alpha}) \right\} \quad (1)$$

Here $V(K)$ is the integration volume of the magnetic system K, A is the "exchange constant", J_s is the above-mentioned saturation polarisation (we use $A \cong 1.3 \times 10^{-6}$ erg/cm and $J_s \cong 1$ Tesla for Py, unless otherwise stated); $\vec{H}^{\mathrm{ext}}$ is the external magnetic field and $\vec{H}^{\mathrm{Dip}}$ the internal dipolar field (also called: "stray-field") which is generated by the magnetic moments of the system according to the magnetostatic equation $\vec{H}^{\mathrm{Dip}}(\vec{r},t) = -\mathrm{grad}\,\phi_m(\vec{r},t)$, with $\nabla^2\phi_m = \frac{1}{\mu_0}\,\mathrm{div}\,(J_s \cdot \vec{\alpha})$ and the corresponding boundary and interface constraints. (Note that at this place, even on a ps time scale, we can safely use the magnetostatic equations without taking into account retardation effects, since e.g. in the time of $\tau = 1$ ps a vacuum electromagnetic wave would traverse a distance of 300 $\mu\,m$, which is far beyond the length scales of the structures considered, [14].)

The dynamic equation of motion corresponding to (1) is

$$\frac{\mathrm{d}\vec{\alpha}}{\mathrm{d}t} = -\gamma_0\, \vec{\alpha} \times \vec{H}^{\mathrm{eff}}\,, \quad (2)$$

where $\gamma_0 = g\frac{|\mu_B|}{\hbar}$ is the "*gyromagnetic ratio*" (μ_B is Bohr's "magneton", $\hbar$ Planck's constant divided by 2π, and g the Landé factor, $g = 2$ for spin magnetism, i.e. in this case γ_0 has the value $1.176 \cdot 10^7$ s^{-1}/Oe), whereas $\vec{H}^{\mathrm{eff}}$ is the space- and time-dependent effective magnetic field, around which the magnetic polarisation precesses, namely

$$\vec{H}^{\mathrm{eff}} = \vec{H}^{\mathrm{ext}} + \vec{H}^{\mathrm{Dip}} + \frac{2A}{J_s}\,\nabla^2\vec{\alpha} - \frac{\alpha_G}{\gamma_0} \cdot \frac{\mathrm{d}\vec{\alpha}}{\mathrm{d}t}\,. \quad (3)$$

Here – as already mentioned – α_G is Gilbert's damping constant, [11]; i.e. the last term in equation (3) describes an isotropic velocity dependent phenomenological damping leading to a gradual decay of the precession amplitude. In principle, and particularly near interfaces, this damping should be anisotropic, see e.g. [15, 16], but in the following this damping anisotropy is neglected, and also the thermal fluctuation

fields, which would be proportional to $(T \cdot \alpha_G)^{\frac{1}{2}}$, are neglected as usual (but see the recent papers of Brown *et al.* and Nowak *et al.*, [17, 18]). Also deviations from cubic symmetry of the magnetic material, which would lead to a more general density of the exchange energy, namely $\sum_{i,j=1}^{3} A_{ij} \frac{\partial \vec{\alpha}}{\partial x_i} \cdot \frac{\partial \vec{\alpha}}{\partial x_j}$, are neglected.

3 Static behaviour of a magnetic dot: Vortex state versus in-plane single-domain state

3.1 Vanishing external field

At first we consider the static behaviour of a flat circular magnetic dot for vanishing external field; in particular we consider the phase boundary between the vortex state and an in-plane single-domain state, [19], minimizing the "Landau-Lifshitz Functional" (1) with the *ansatz*

$$\begin{aligned} \alpha_x(r) &= -\sin\varphi(r) \cdot (1-\alpha_z^2(r))^{\frac{1}{2}} \\ \alpha_y(r) &= +\cos\varphi(r) \cdot (1-\alpha_z^2(r))^{\frac{1}{2}} \end{aligned} \tag{4}$$

Our special ansatz for the 'profile function' $\alpha_z(r)$ is an improved version of an approximation by Feldtkeller and Thomas, [20]), led by the following considerations:

For $r \ll l_m$, where $l_m := (\frac{2A\mu_0}{J_s^2})^{\frac{1}{2}}$ is the 'magnetic exchange length', one expects the behaviour $\alpha_z(r) = 1 - \text{const.} \cdot r^2 - ...$ (where the dots denote higher-order terms); beyond that range one will observe an exponential spatial dependence with decay length l_m, while asymptotically for $r \gg l_m$ some kind of 'Mexican Hat' behaviour will apply, i.e. after the pronounced exponential decay $\alpha_z(r)$ should become negative and approach the r-axis from negative values. However, this negative part should be proportional to the magnetic moment of the central part of the dot, i.e. $\sim J_s \pi l_m^2 t_h$, and therefore it vanishes $\propto t_h$ for very flat dots.

(Our *ansatz* for $\alpha_z(\vec{r})$, see below, is more accurate than that of eq. (5) of Usov and Peschany, [7], who neglect the magnetostatic energy generated by the vortex core completely to obtain their simplified profile function, which contains a singularity of the derivative at the so-called core radius and is constant for larger r, i.e. it does not contain the tail nor the negative part of the profile. Our calculation is also

more accurate, see the results, than that of Guslienko and Metlov, [6], and Guslienko *et al.*, [21], who take the magnetostatic field produced by the vortex core into account, but use basically the simplified core profile of [7] instead of the more correct one of (5) below.)

In any case, as a systematic approximation, expanding the ansatz of Feldtkeller and Thomas, [20], we use in eq. (4):

$$\alpha_z(r) \equiv c \cdot e^{-\frac{r^2}{l_m^2}} + (1-c) \cdot e^{-\frac{r^2}{4l_m^2}}, \tag{5}$$

where c depends on the thickness of the sample and is obtained by an energy-fitting procedure leading to

$$c \approx -0.188 + 0.708 \cdot (1 + 0.2 \cdot T_h + 0.0278 \cdot T_h^2)^{-1}\,. \tag{6}$$

Here $T_h := \frac{t_h}{l_m}$ is the reduced thickness of our structures. Note that $c \approx 0.5$ for very flat dots ($t_h \ll R$). (Eqs. (5) and (6) are of course only approximately valid, since 'Mexican hat profiles', which one would get for thicker dots, are explicitly excluded for $-0.188 \leq c \leq 0.52$.)

In fact, the gross behaviour of the profile function for our flat structure is given by the above-mentioned ansatz (5): This is exemplified in Fig. 1, where the results of a numerical simulation of $\alpha_z(r)$, performed with the OOMMF program, [22], for flat circular permalloy structures with $R = 175.5$ nm and a thickness of $t_h = 6$ nm, are compared with (5) and (6). Details are given in Fig. 1a and in the corresponding figure caption. In Fig. 1b an effective radius R_{eff} of the central region of the vortex is presented as a function of the reduced thickness T_h. This effective radius R_{eff} is defined by the equation $R_{\text{eff}} = \frac{\pi}{2} \cdot \frac{1}{\left(\frac{\mathrm{d}\theta}{\mathrm{d}r}|_{r=0}\right)}$, taking into account the fact that the polar angle θ of the magnetic polarisation is zero rsp. $\frac{\pi}{2}$ in the vortex center rsp. far from it. With (5) one gets $R_{\text{eff}} \cong \frac{\pi}{\sqrt{2+6\cdot c}} \cdot l_m$, which is plotted in Fig. 1b. This means that R_{eff} is approximately between $1.5\,l_m$ and $3\,l_m$ depending on the thickness t_h.

Our ansatz $\alpha_z(r)$, eq. (5), for the above-mentioned profile function leads to *analytical* formulae for the exchange energy density $f^{\text{exch}} = \frac{A}{V} \int\limits_V \sum\limits_{i=1}^{3} (\frac{\partial \vec{\alpha}}{\partial x_i})^2 \,\mathrm{d}V$, and we obtain for thin dots with $c = 0.5$ approximately: $f^{\text{exch}} \approx \frac{2A}{R^2} \cdot [2.67 + \ln \frac{R}{5l_m}]$.

For circular single-domain dots with homogeneous magnetization there is only the stray-field energy. For in-plane states, magnetic poles

arise exclusively at the side-face S (i.e. $r \equiv R$), and we obtain for the stray-field energy density

$$f^{\mathrm{Dip}} := \frac{1}{V} \cdot \frac{J_s^2}{8\pi\mu_0} \int\limits_S \int\limits_{S'} \frac{(\vec{\alpha}(\vec{r}) \cdot \vec{n}(\vec{r})) \cdot (\vec{\alpha}(\vec{r}^{\,\prime}) \cdot \vec{n}(\vec{r}^{\,\prime}))}{|\vec{r} - \vec{r}^{\,\prime}|}) \, \mathrm{d}^2 S \, \mathrm{d}^2 S^{\prime} \ . \quad (7)$$

By numerical evaluation, followed by a fit, we get: $f^{\mathrm{Dip}} \approx \frac{J_s^2}{8\pi\mu_0} \cdot [2.41 \cdot \ln(1 + 5.31\,(\frac{t_h}{2R})^{0.88})]$.

From these results one obtains for the critical thickness $t_c(R)$, where the energies of the vortex state and the in-plane single-domain states agree, with the ansatz (5):

$$t_c(R) \cong 2\,R \cdot \left\{ \frac{1}{5.31} \cdot \{ \exp\left(\frac{8\pi}{2.41} \cdot \frac{l_m^2}{R^2} \cdot [2.67 + \ln \frac{R}{5 l_m} + 0.5] \right) - 1 \} \right\}^{\frac{1}{0.88}} . \quad (8)$$

Here the term ~ 0.5 comes from the dipolar energy of the central part of the vortex.

In Fig. 2, this result for the critical thickness is plotted against R (the solid line) and compared with the results of an unpublished simplified calculation, (see [23, 24], the dashed line, i.e. $t_{c,0}(R)$), where the fact that in the center of the vortex α_z is different from zero has been totally neglected (yielding a wrong asymptotics for $R \ll l_m$), and where the magnetostatic energy has been calculated by replacing the circular dot of radius R and thickness t_h by a prolate ellipsoid. It turns out that this simple calculation is not bad and captures the essentials, although there is still a significant discrepancy w.r.t. the direct numerical simulation e.g. by the OOMMF program. In contrast the better results with our ansatz (5) for the profile functions can hardly be distinguished, to the accuracy of the plot, from the results of the OOMMF simulation.

(Additionally, Metlov and Guslienko, in their recent paper [5] on thicker cylindrical dots, have determined the transition line between in-plane and out-of-plane single domain states, see Fig. 2 in [5]. However for our flat dots with $t_h \ll R$ this addition is not important. In fact, in our Fig. 2, the additional phase boundary would be represented by a very steep line almost parallel to the abscissa axis, which would terminate at our 'solid line' phase boundary at a thickness of ~ 43 nm. This is far beyond the thicknesses we consider.)

3.2 In-plane external fields

For in-plane external fields, the vortex deforms, and its center shifts by an amount Δ (in x-direction, if the external field is applied in the y-direction; actually, see Fig. 8, below, the dynamic behaviour is more complicated). For simplicity, in the following approximation we only take into account the *shift*. Here both $\Delta < R$ and also $\Delta \geq R$ are considered, see below). With this approximation we minimize the Landau-Lifshitz functional. For the 'stray-field energy density' we again have to evaluate (7) with the (fictitious) magnetic poles at the side-face S; additionally there is now the Zeeman energy density

$$f^{\text{Zeeman}} = -J_s |H^{\text{ext}}| \cdot \frac{\Gamma(R, \Delta, l_m, c)}{\pi R^2}\,, \tag{9}$$

where $\Gamma(R, \Delta, l_m, c)$ is a function of the parameters R, Δ, l_m and c. Note that – as already mentioned – Δ can be larger than R, although one expects that the transition from the vortex state to the in-plane single-domain state just happens in the region $\Delta \approx R$.

In Fig. 3, again for a circular Py dot of $R = 150$ nm and $t_h = 4$ nm in an external in-plane field of $H_y^{\text{ext}} = 100$ Oe, the energy densities (dipole energy, Zeeman energy, exchange energy, and total energy) are plotted as a function of the shift parameter Δ. The equilibrium position of the vortex center would correspond to the minimum of the total energy, which appears at $\Delta \approx 0.4\,R$. With increasing Δ ($\rightarrow R$), in Fig. 3 there is an *energy barrier*, separating the in-plane single-domain state (i.e. $\Delta \gg R$) from the deformed vortex state (i.e. $\Delta < R$). However this energy barrier depends on H_y^{ext}, and with increasing H_y^{ext} it decays to zero as shown in Fig. 4.

Fig. 4 yields quantitative results for the 'annihilation fields' of the vortex state rsp. for the energy barrier separating the vortex state from the in-plane single-domain state, if the in-plane external field is not strong enough for the transition. Since the deformation of the vortex during the shift is neglected in our approximation, this energy barrier is overestimated. In any case, near 'rough boundaries' the actual behaviour will be too complex for a simple calculation, see [25].

In Fig. 5, we compare our calculations with experimental results for the annihilation fields of flat circular Py samples, plotted over the double reciprocal aspect ratio $2R/t_h$, see [26]. In our calculation we

have used the experimental values $A = 1.3 \times 10^{-6}$ erg/ccm, $J_s = 0.9676$ Tesla, zero anisotropy, and two thicknesses ($t_h = 15$ nm and $t_h = 8.3$ nm). As can be seen from the figure, in agreement with the above-mentioned arguments, our theoretical estimates are systematically $\approx 20 - 30$ % too high, but a large part of the deviation is probably due to the fact that in the experiments a non-neglegible perpendicular field component was present, [27]; moreover, since the experiments are at room temperature, the influence of thermal fields may also have been non-neglegible, see ref. [16, 28]. In any case, in the paper of Guslienko and Metlov, [6], who also perform a comparison with the experiments of [26], the theoretical results are significantly overestimated at small values of R/t_h, contrasted with our Fig. 5. The discrepancy is due to the fact that the authors of [6] use basically the simplified profile function of Usov and Peschany, [7], which should not be applied for $R \lesssim t_h$. But globally, i.e. averaged over all values of R/t_h, in [6], the agreement between the calculated vortex annihilation fields and the experiments looks better than that one presented in our Fig. 5, in spite of the drastic overestimation at small values.

4 Dynamics

This topic is particularly emphasized in our paper; to use both the *vorticity* and the *central polarisation* of flat circular dots for information processing one should be able to switch both properties reliably and independently, and – of course – fast, i.e. significantly below ns time scales.

Unfortunately, the vorticity of the static magnetic state cannot be directly influenced experimentally with *circular* dots. However, M. Schneider *et al.* have shown how one can easily influence the vorticity of the magnetic state by using dots, which are not perfectly circular, cutting-off a segment of the structure, see [3]. This refers to static or quasi-static conditions. *But in the following we consider fast dynamic changes, at first by time-dependent in-plane fields, and then by time-dependent perpendicular fields* :

4.1 Time-dependent in-plane fields

As usual, we consider a circular Py dot ($A = 1.3 \times 10^{-6}$ erg/ccm, $J_s = 1.08$ T, neglegible anisotropy) with $R = 150$ nm and 4 nm thickness. Without external field, the dot is in a stable vortex state. At time $t = 0$, an in-plane external field $H_y^{\rm ext}$ is applied, and the 'critical duration' $t_{\rm crit}$ is determined, i.e. the time until the vortex has been shifted to the edge of the dot ($\Delta = R$), so that the vortex state is either 'lost' to an in-plane single-domain state, $\Delta \geq R$, or restored ($\Delta \to 0$) after the field $H_y^{\rm ext}$ is switched off. The results (which have been obtained by computer simulations with the OOMMF code, [22]) are presented in Fig. 6; they depend on Gilbert's damping parameter α_G in a rather subtle way (see below). At first, we see from this figure that to reach critical times below $t = 1$ ns one needs quite strong external fields, namely $H_y^{\rm ext} \gtrsim 300$ Oe to get below 800 ps, and $\gtrsim 500$ Oe to get below 600 ps. Moreover, the information contained in the polarisation of the vortex center is only preserved for unrealistically large α_G (e.g. for $\alpha_G = 1$ the vortex center is only stable for fields $H_y^{\rm ext} < 1100$ Oe, i.e. up to the end-point of the lowest curve in Fig. 6.) For $\alpha_G = 0.5$ the corresponding (second-lowest) curve in Fig. 6 ends already at $H_y^{\rm ext} = 650$ Oe with $t_{\rm crit} = 500$ ps, and for $\alpha_G = 0.01$ we have only obtained one point in Fig. 6, namely with $t_{\rm crit} = 1000$ ps and $H_y^{\rm ext} = 200$ Oe. If the vortex state is 'lost' to an in-plane single-domain state by the application of the in-plane field $H_y^{\rm ext}$, one would need roughly at least another 'critical duration' to generate a new vortex state beginning from the boundary of the circular dot and propagating the core of the new vortex to the center; maybe this new vortex has inverted vorticity, inverted according to the systematic but slow prescription of [3, 29]. In any case, this vorticity-switching would be too slow, and too complex.

In fact, one sees from Fig. 7, where in an (α_G, $H_y^{\rm ext}$)–plane the boundary line separating stable and unstable regions of the (deformed) vortex state is plotted, that for realistically small values of α_G the vortex center is unstable for fields above 200 Oe, i.e. the independent information contained in the *central polarisation* of the vortex gets lost by the application of $H_y^{\rm ext}$: Stability of this 'polarisation information' can only be obtained for smaller in-plane fields $H_y^{\rm ext}$, which also means 'critical times' larger than 1 ns.

In the next figure, Fig. 8, which corresponds to some kind of '*movie*

sequence', the particular case of $\alpha_G = 0.02$ is considered in detail, for $H_y^{\rm ext} = 300$ Oe. (The observation that the vortex core moves in the 'north-east' direction, although from the fact that the switching-field is applied in the y-direction one would expect that it should move exactly 'eastwards', comes from the following: In the first ~ 100 picoseconds the vortex core, in fact, starts moving to the right, but at the same time some kind of 180^o domain wall is formed on the segment between $x = 0$ and $x = R$; under the influence of the H_y-field this domain wall tends to move upwards, and after 600 ps it can still be identified in Fig. 8 to the r.h.s. of the vortex core. In any case, since the 'domain wall segment' is fixed to the (slower) vortex core, the "north-east" motion of the core results, as a consequence of the complicated coupling between all spins in course of the dynamics. Further details are only seen if the 'movie' corresponding to Fig. 8 is observed on a shorter time-scale.)

The total simulation time of Fig. 8 is 1.5 ns: One concludes that vorticity annihilation is interesting and complicated, but rather slow ($t_{\rm crit} \approx 1.5$ ns); particularly, the information contained in the central polarisation is lost by applying the field $H_y^{\rm ext}$ for the critical duration, and one is far from simply 'switching' the vorticity. (These conclusions would also apply for larger values of α_G, although for $\alpha_G = 1$, which is unrealistically large, one would gain a factor of 3 in speed.)

As a consequence, for vorticity-switching one should not use in-plane fields, but instead one should work with perpendicular fields, as discussed in the following.

4.2 Time-dependent perpendicular fields

We have finally performed simulations, starting from the planar equilibrium vortex configuration, with pulsed external 'switching fields' which are now *perpendicular* to the plane. We consider the same structure as before. The applied field pulse was very strong, $B_z^{\rm ext} = \mu_0 H_z^{\rm ext} = 0.5$ T, i.e. $H_z^{\rm ext} \hat{=} 5000$ Oe, but also very short (see below). The Gilbert damping was assumed to be as small as in Fig. 8, i.e. $\alpha_G = 0.02$, but the pulse time of $H_z^{\rm ext}$ was only 42 ps, i.e. only a small fraction of the total simulation time of the corresponding 'movie sequence', which we calculated for that example. This time the vorticity is really inverted, and the switching is very fast, 42 ps, and without "ringing" after the end of the field-pulse.

In Fig. 9 we consider the effective 'switching time' $t_{\rm sw} = t_{\frac{1}{2}}$, i.e. the time needed to turn around the spins – in a spatial average – by 180 degrees, systematically as a function of $H_z^{\rm ext}$. For vanishing damping this corresponds to a gyromagnetic precession by an angle π, i.e. $t_{\frac{1}{2}} = \frac{\pi}{|\gamma_0| \cdot H_z^{\rm ext}}$. This is shown in Fig. 10, which presents results from the first part of our 'movie'. After a duration of $t_{\frac{1}{2}}$, 42 ps in our case, the field is switched off; the system then 'wiggles' around the new equilibrium vortex state and gets slowly into equilibrium after several ns. *But the 'wiggles' are small enough that the new equilibrium state can be clearly recognized already after* 42 *ps, although the system is still far from equilibrium*, [30].

(Note that in Fig. 10 the exchange energy does not change with time, in contrast to the magnetostatic energy, although after ~ 21 ps the transient spin configuration has changed from a vortex state to a 'hedgehog state'; this invariance of the exchange energy is in agreement with a 'topological statement' of W. Döring, [31].)

In Fig. 11, the 'wiggling' of the spatial average of α_z is presented. Finally in Fig. 12 we plot, what happens to the polarisation of the vortex center under the influence of a 'tilted vertical field pulse', involving a strong perpendicular component $H_z^{\rm ext} = -1000$ Oe, applied between $t = 0$ and 60 ps, accompanied by a simultaneous weaker in-plane pulse of $H_y^{\rm ext} = 150$ Oe between $t = 0$ and $t = 30$ ps. We find that at first the central polarisation is inverted from (+) to (-), but then it returns to the starting state (+). In fact, we find it difficult to control the central polarisation independently and with similar speed as the vorticity.

That very strong vertical fields in the kOe range are necessary for polarity-switching of the vortex core is also found in a recent letter of Kikuchi *et al.*, [32].

We have seen that the fast switching of the vorticity by vertical fields works successful, but the 'switching field pulses' are in fact very large in strength, ≈ 5000 *Oe, and very short in duration,* ≈ 40 *ps. However, concerning the independent switching of the polarisation of the center of the vortex, we always have found (for realistically small values of* α_G*) that the central polarisation – in contrast to the vorticity – can hardly be controlled even by strong field pulses oriented perpendicular to the plane; therefore in this case we are unsuccessful and do not plot the results of our simulations.*

4.3 Vortex structure in flat circular dots: discussion

Here we collect our results for the flat circular Permalloy (Py) dots considered in this section 4:

1. The switching fields are quite large, i.e. necessary values are higher than 300 Oersteds (for in-plane fields), and 5000 Oersteds for the case of perpendicular fields.

2. For realistic values of the Gilbert damping parameter α_G, see [11], only the *vorticity* can be reliably switched, [33], but not the *central polarisation* of the vortex core.

3. The time scale necessary for the precessional switching of the vorticity is very short, $\tau \sim 40$ ps, for the case of perpendicular field pulses. In that case, after the switching the magnetization "wiggles" slightly, i.e. there are relatively small oscillations, below $\pm 10\%$, around the new equilibrium. These small precessional oscillations decay rather slowly on a much larger ns time scale. *But principally the information contained in the new state can already be obtained after 40 ps with sufficiently strong perpendicular field pulses without necessity to suppress the 'wiggling'*, [34].

4. For the case of in-plane switching fields the field strengths for the dynamic annihilation of the vortex state are an order of magnitude lower, $B_y^{\text{ext}} \sim 300$ Oersteds, and they need not to be pulsed; but the time scales for vortex-switching with in-plane fields are also an order of magnitude slower, namely $\gtrsim 500$ ps, [35].

5 Vortex structure in flat circular 'nano-rings'

As a consequence, at the end, we dismiss the vortex center totally, although this implies the definite loss of the the possibility, to manipulate a second bit. We consider flat circular 'nano-rings' with an inner radius R_1 and an outer radius R_2. In this case, see Fig. 13, with increasing R_1 the energy density of the vortex state decreases, while that of the homogeneous in-plane state ('single-domain state') increases significantly, i.e. the stability of the vortex state is enhanced.

At the same time the switching of the vorticity by perpendicular field pulses is hardly influenced by the size of R_1: In Fig. 14 we present simulations for Py dots with $R_2 = 150$ nm and $t_h = 4$ nm, comparing our former results for $R_1 = 0$ with similar 'ring results' for $R_1 = 50$ nm, as a function of the switching field $H_z^{\rm ext}$. Obviously the switching time $t_{\frac{1}{2}}$ is practically not changed.

6 Conclusions

Within the framework of the Landau-Lifshitz-Gilbert equation, using permalloy parameters, we have studied the statics and dynamics of flat circular magnetic nano-structures with an in-plane magnetic vortex configuration putting particular emphasis on the (perpendicular) *polarisation* of the vortex center (which may be shifted with respect to the center of the circle), and on the (in-plane) *vorticity* of the magnetic state. Studying switching processes induced by in-plane and out-of-plane field pulses, we find that it is possible to switch the *vorticity* of the magnetic dot on an ultra-short time scale of 40 ps with strong enough and short enough perpendicular external field pulses (strength $\mu_0 H_z^{\rm ext} \approx 0.5$ T; duration ≈ 40 ps); but for realistic values of the Gilbert damping constant α_G, only the *vorticity* can be switched this fast, but not the magnetic polarisation $\alpha_z = \pm 1$ of the vortex core, so that it is better to dismiss the center of the circular structures totally, concentrating instead on flat nano-rings, i.e. with an inner radius R_1 and an outer radius R_2. In such nano-rings, the stability of the vortex state is enhanced, and concerning the switching of the vorticity, they have similar properties as circular ones, i.e. with $R_1 = 0$.

For in-plane fields, the field strength need only to be $\gtrsim 200$ Oersteds, but the time scales of vorticity-switching are $\gtrsim 1$ ns; the vortex center is typically unstable, i.e. the topology of the state is changed from a 'deformed vortex state' to a 'deformed in-plane single-domain state', if in-plane fields of the 'critical duration' are applied. So the case of 'in-plane vortex switching fields' should be dismissed rightaway for circular dots.

Acknowledgements

We acknowledge stimulating discussions with C. Back, G. Bayreuther, H. Hoffmann, M. Schneider, and J. Zweck.

References

[1] G.A. Prinz, J. Magn. Magn. Mater. **200** (1999) 57

[2] R. Cowburn, M.E. Welland, Science **287** (2000) 1466

[3] M. Schneider, H. Hoffmann, J. Zweck, Appl. Phys. Lett. **79** (2001) 3113; M. Schneider, PhD thesis, University of Regensburg 2002

[4] C. A. Ross, M. Hwang, M. Shima, J.Y. Cheng, M. Farhoud, T.A. Savas, Henry L. Smith, W. Schwarzacher, F.M. Ross, M. Redjdad, F.B. Humphrey, Phys. Rev. B **65** (2002) 144417

[5] Konstantin L. Metlov, Konstantin Yu. Guslienko, J. Mag. Magn. Mater. 242-245 (2002) 1015.

[6] Konstantin Yu. Guslienko, Konstantin L. Metlov, Phys. Rev. B **63** 100403(R). – In this reference, the authors did not directly use the Usov model of shifted vortex, [7], but some other model based on a conformal mapping of the Usov magnetization distribution.

[7] N.A. Usov, S.E. Peschany, J. Magn. Magn. Mater. **118** (1993) L290

[8] Th. Gerrits, H.A.M. van den Berg, J. Hohlfeld, L. Bär, Th. Rasing, Nature **418** (2002) 509

[9] V. Novosad, M. Grimsditch, K.Yu. Guslienko, P. Vavassori, Y. Otani, S.D. Bader, Phys. Rev. B **66** (2002) 052407

[10] J. Raabe, R. Pulwey, R. Sattler, T. Schweinböck, J. Zweck, D. Weiss, J. Appl. Phys. **88** (2000) 4437

[11] T.L. Gilbert, Phys. Rev. **100** (1955) 1243

[12] A. Aharoni, *Introduction to the theory of ferromagnetism*; Oxford, Clarendon Press 1996

[13] A. Hubert, R. Schäfer, *Magnetic Domains*; Berlin, Heidelberg, New York, Springer 1998

[14] It is perhaps not generally known that in polarizable matter the transient electrodynamics following a short perturbation is determined by retardation effects involving the vacuum velocity of light, and not by the slower velocity of stationary light waves in that matter.

[15] V. L. Safonov, e-print cond-mat/0111566

[16] A.A. Fraermann, S.A. Gusev, L.A. Mazov, I.M. Nevedov, Yu.N. Nozdrin, Phys. Rev. B **65** (2002) 064424
The authors show among other points in Fig. 5 of their paper that the magnetization curves generated by rectangular lattices of permalloy nanoparticles show significant differences at 4.2 K and 77 K, respectively, which is attributed to thermal field fluctuations.

[17] G. Brown, M.A. Novotny,, P.A. Rikvold, Physica B **306** (2001) 117; Phys. Rev. B **64** (2001) 134422

[18] D. Hinzke, U. Nowak, J. Appl. Phys. **85** (1999) 4337

[19] The out-of-plane single domain state, which would be energetically very unfavourable, does not play a role for our flat permalloy dots.

[20] E. Feldtkeller, H. Thomas, Phys. kond. Materie **4** (1965) 8

[21] K.Yu. Guslienko, V. Novosad, Y. Otani, H. Shima, K. Fukamichi, Phys. Rev. B **65** (2002) 024414

[22] Micromagnetic simulation software package "OOMMF" ($\hat{=}$ 'object-oriented micromagnetic framework'),
http://math.nist.gov/oommf

[23] H. Hoffmann, private communication

[24] M. Schneider, H. Hoffmann, J. Zweck, Appl. Phys. Lett. **77** (2000) 2909

[25] R. P. Cowburn, J. Phys. D: Appl, Phys. **33** (2000) R1

[26] M. Schneider, private communication

[27] M. Rahm, private communication

[28] J. Li, J. Shi, S. Tehrani, Appl. Phys. Lett. **79** (2001) 3821

[29] The slowness of the 'switching process' of a vortex state by in-plane fields $H_y^{\rm ext}$ is also shown in a recent paper by N.A. Usov, L.G. Kurkina, J. Magn. Magn. Mater. **242-245 (P2)** (2002) 1005

[30] This relative 'harmlessness' of the "wiggling" in the vorticity switching is in contrast to the 'severeness' of the "ringing" phenomenon in the precessional switching of single-domain states, where "ringing" poses severe problems; see the contributions in [8, 34, 35].

[31] W. Döring, J. Appl. Phys. **19** (1968) 1006

[32] N. Kikuchi, S. Okamoto, O. Kitami, Y. Shimada, S.G. Kim. Y. Otani, K. Fukamichi, J. Appl. Phys. **90** (2001) 6548

[33] The Gilbert parameter for Py is very small, $\alpha_G = 0.008$, and at the interfaces of thin films or trilayers this is only enhanced to typical values around $a_G \approx 0.1$ or below, [36].

[34] This last-mentioned property is not in contrast to the recent paper of Gerrits *et al.*, [8], who discuss the dynamics of an in-plane single-domain switching process, which is slower by a factor of five than our vortex switching, but works with smaller magnetic fields for the switching, with additional suppression of the "ringing" in the precessional switching dynamics by a second field pulse; see also H.W. Schumacher, C. Chappert, P. Crozat, R.C. Sousa, P.P. Freitas, M. Bauer, Appl. Phys. Lett. **80** (2002) 3781

[35] Recently one of us (R. H.) has studied the switching of in-plane magnetized flat single-domain dots by out-of-plane magnetic switching field pulses with a particular shape and found a switching time of ~ 200 ps (with minimal "ringing"), with $H_z(t)$ in the kOe range and below; R. Höllinger, to be published.

[36] Y. Tserkovnyak, A. Brataas, G. E. W. Bauer, Phys. Rev. Lett. **88** (2002) 117601

Figures and Figure Captions

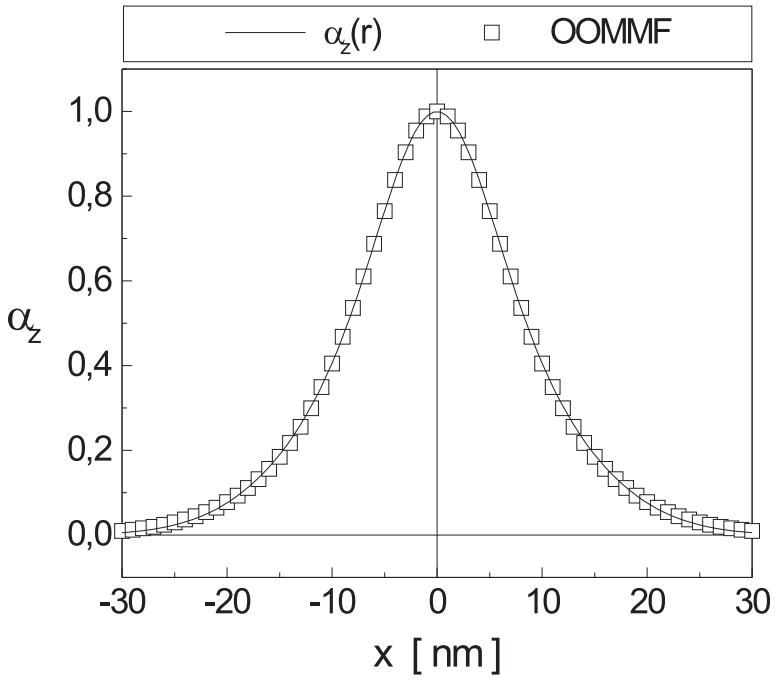

Fig.1a: The 'profile function' $\alpha_z(r)$ as given by our analytical ansatz is compared with results of the direct numerical simulation by the OOMMF code. Material parameters: Permalloy. The radius of the circular dot considered is 175.5 nm, the height is 6 nm.

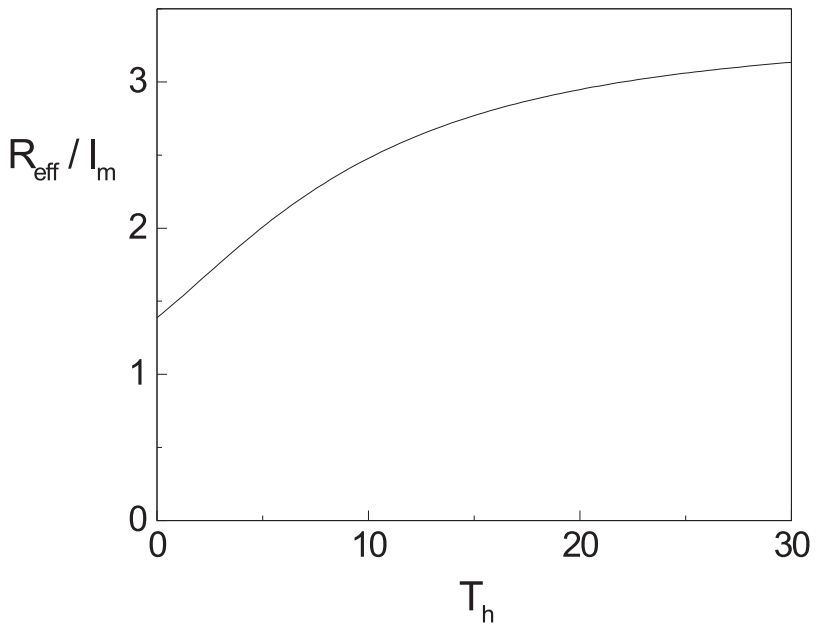

Fig.1b: The effective radius R_{eff} of the vortex core is presented over the reduced thickness $T_h := \frac{t_h}{l_m}$ of the circular dot, in units of the magnetic exchange length l_m. Material parameters: Py, as in Fig. 1a.

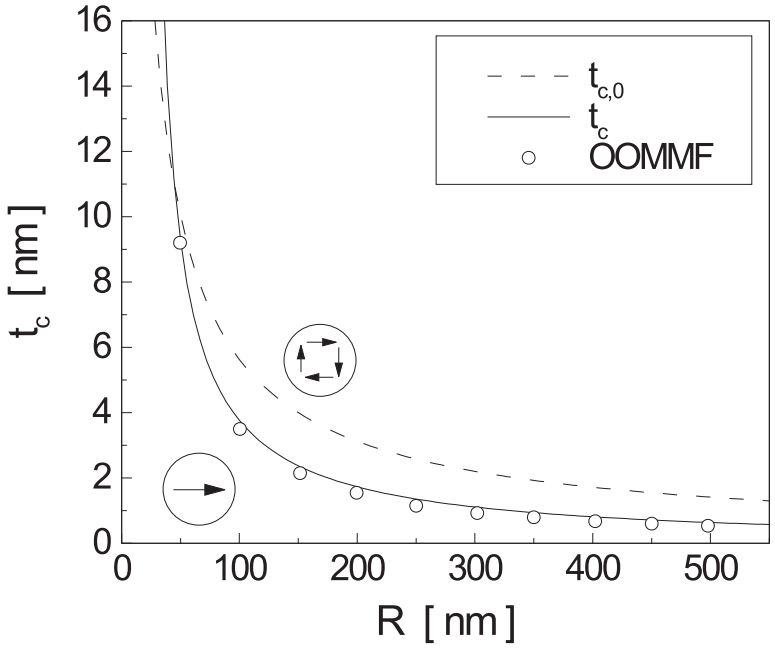

Figure 2: The critical thickness $t_c(R)$, i.e. the line which separates the stability ranges of the vortex state from that of the in-plane single-domain state, is presented as a function of the radius R of the circular dot. Parameters of Permalloy material are used. The solid line describes our results, as given in the text; the dashed line presents the simplified approximation $t_{c,0}(R)$, also described in the text, and the circles describes the results of a numerical calculation with the OOMMF code. (Besides, the additional phase transition line separating the out-of-plane single-domain state from the in-plane single domain state would in the present plot almost coincide with the abscissa axis.)

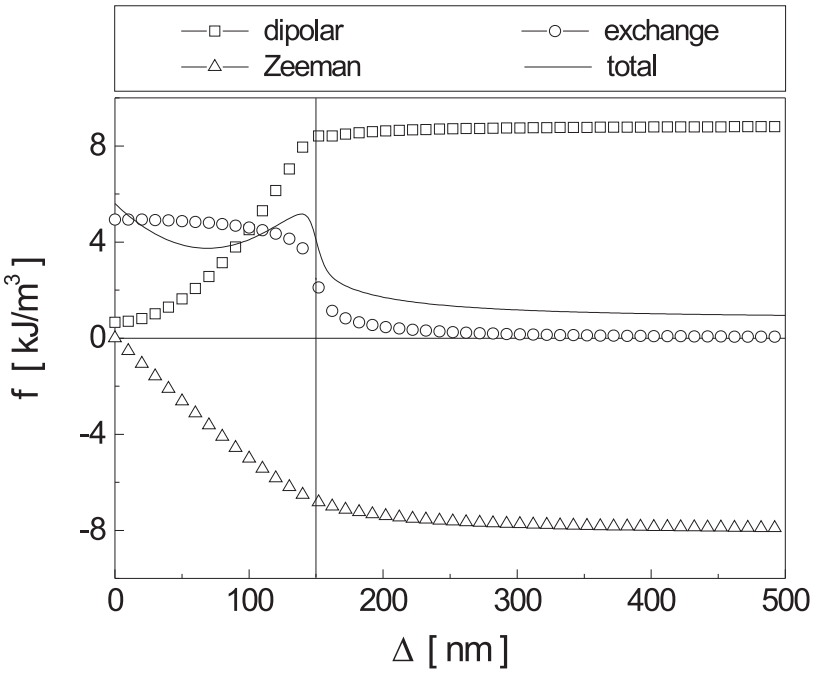

Figure 3: The total energy density f (the solid line), and the partial energy densities of the dipolar energy (squares), exchange energy (diamonds) and Zeeman energy (triangles)) for the vortex state in a circular permalloy dot of radius $R = 150$ nm (note the vertical line) and thickness $t_h = 4$ nm are presented as a function of the shift Δ of the vortex core; for more details see the text

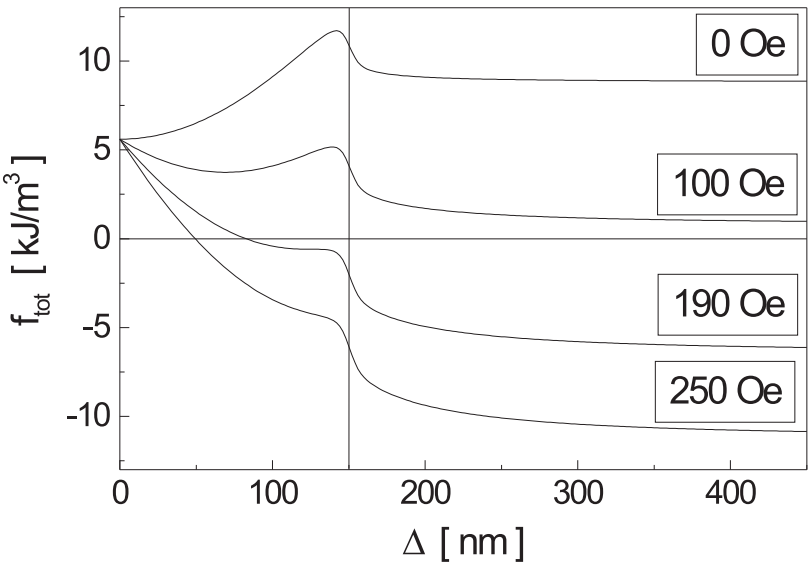

Figure 4: For different values of the external in-plane Zeeman field the density f_{tot} of the total energy of Fig. 3 is presented against the shift Δ of the vortex core. One can see that for strong enough Zeeman fields ($H_y^{\mathrm{ext}} \geq 190$ Oe) there is no longer a local minimum, i.e. the vortex vanishes ($\Delta \to \infty$), which means a transition to a single-domain state. The vertical line denotes the radius R of the circular dot.

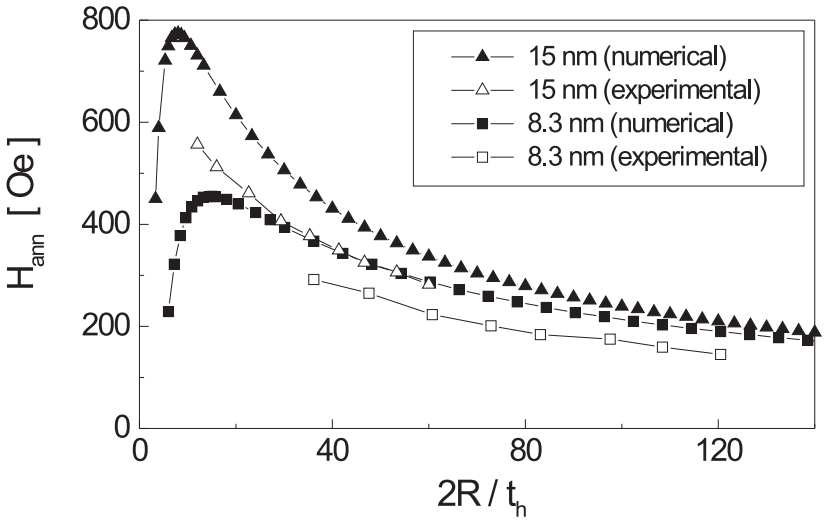

Figure 5: For Py dots of thickness $t_h = 15$ nm and 8.3 nm, respectively, experimental results, and our theoretical results, for the in-plane annihilation fields of the vortex state are presented over the double reciprocal aspect ratio $2R/t_h$ of the dot.

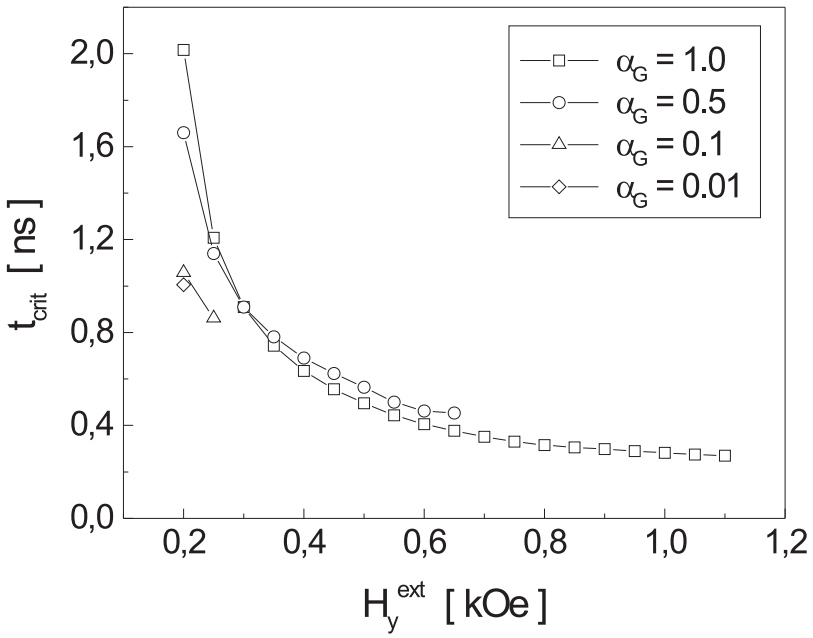

Figure 6: The critical time t_c for dynamic annihilation of the vortex state by in-plane fields $H_y^{\rm ext}$ is presented against $H_y^{\rm ext}$ for different values of the Gilbert damping α_G. For further details see the text.

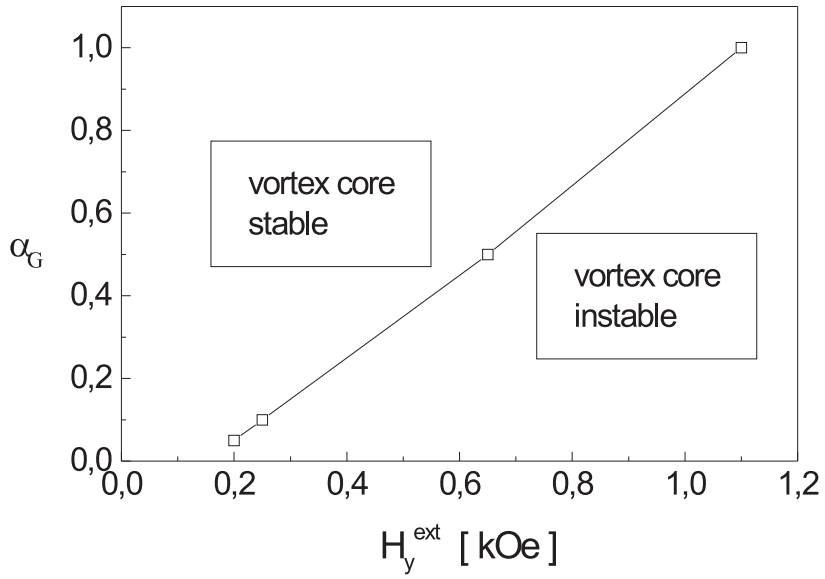

Figure 7: The line separating the dynamic stability and instability regions for dynamic annihilation of the vortex core by in-plane fields, as in the preceding figure, is presented in an $(\alpha_G, H_y^{\rm ext})$ plane, where α_G is Gilbert's damping parameter and $H_y^{\rm ext}$ the in-plane 'switching field'.

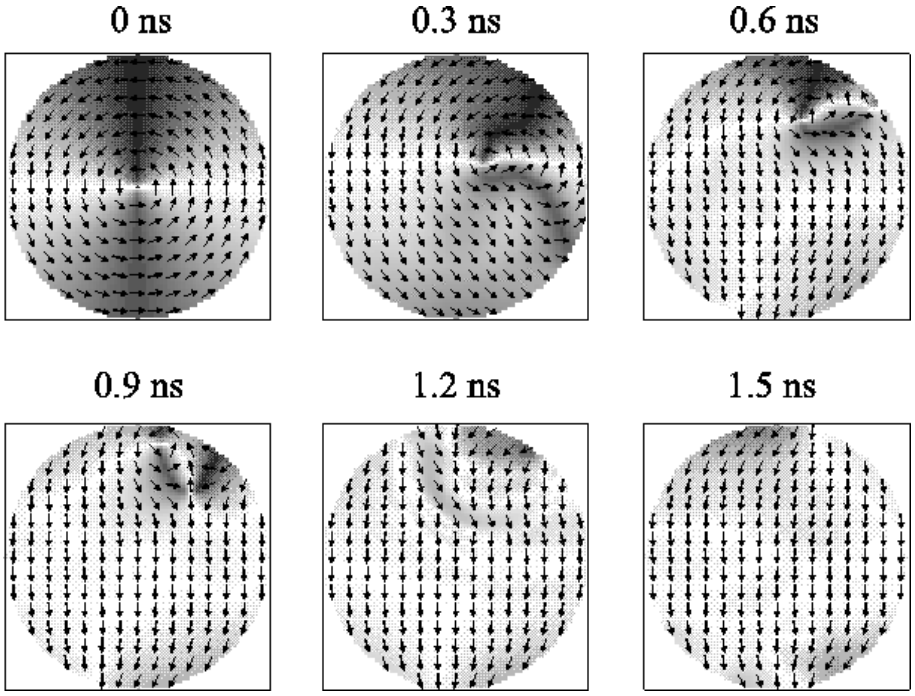

Figure 8: This 'movie sequence' presents the annihilation of a vortex state by an in-plane field. This is a rather slow process, which needs at least 1.5 ns, although the in-plane field is as strong as 300 Oe . Gilbert's damping parameter has been assumed to be $\alpha_G = 0.02$

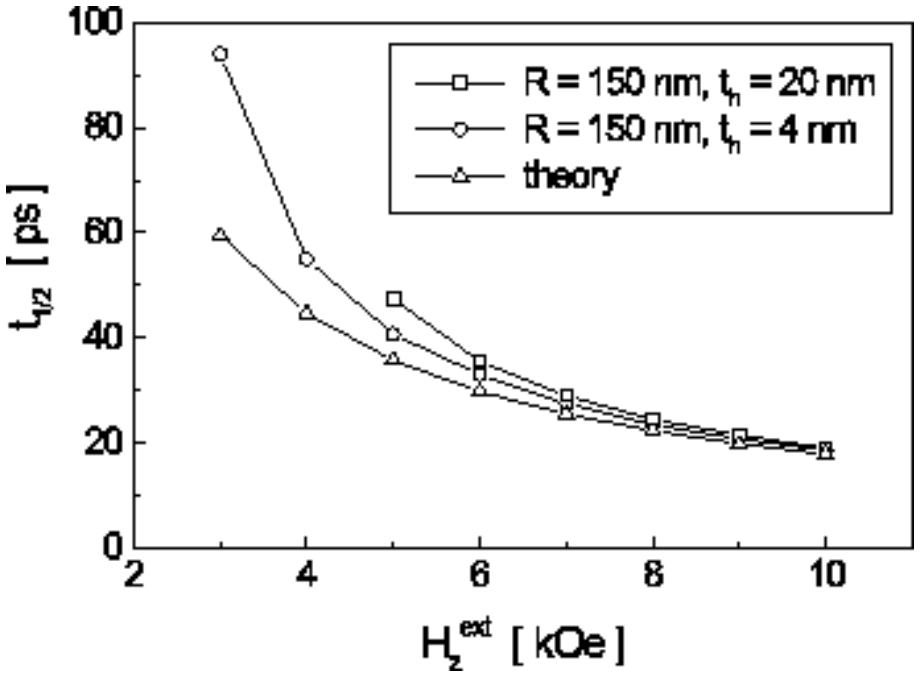

Figure 9: This plot presents the typical 'switching time' $t_{1/2}$ of a vortex state by a pulsed perpendicular field $H_z^{\rm ext}$. This is a very fast process, which needs typically only ~ 40 ps, but the necessary strength of the field is very large, ~ 5000 Oe. Gilbert's damping parameter has been assumed to be $\alpha_G = 0.02$. "Theory" means the simple result $t_{1/2} = \pi/(|\gamma_0| H_z^{\rm ext})$; the other results are from OOMMF-simulations.

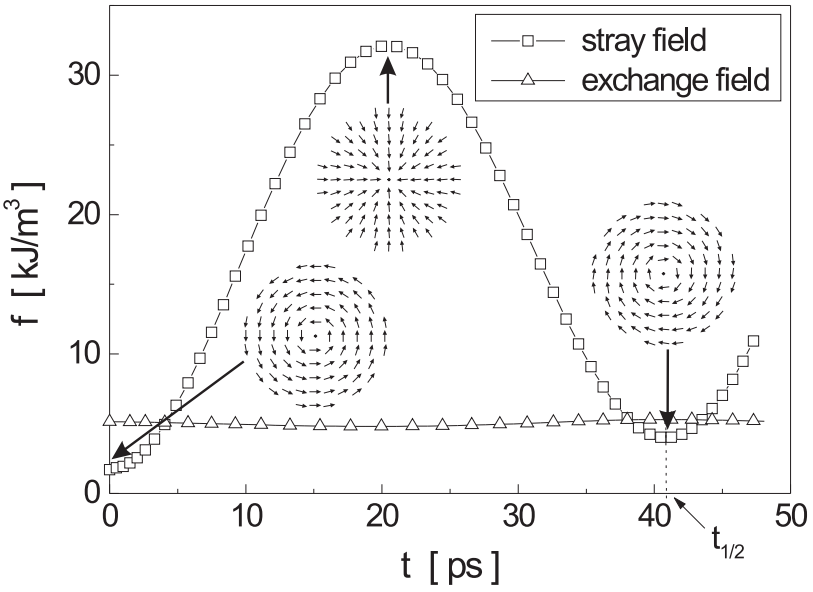

Figure 10: This plot shows details of the fast switching of the vorticity of our flat circular Permalloy dot of radius $R = 150$ nm and thickness $t_h = 4$ nm by a pulsed vertical field of $H_z^{\text{ext}} = 5000$ Oe. The energy densities f of the dipolar energy ('stray-field') and of the exchange energy are presented over the time for the first 50 ps after the start of the perpendicular field pulse, which lasts from $t = 0$ to $t = 42$ ps.

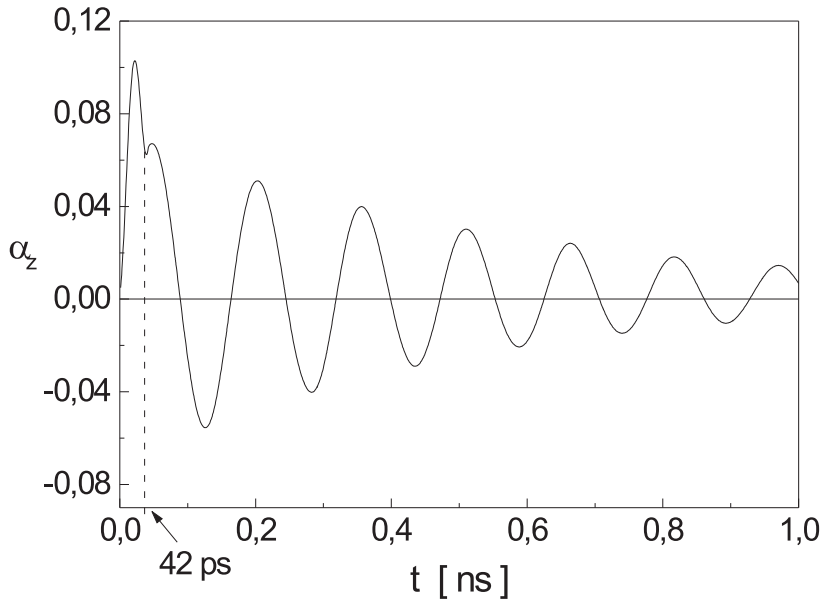

Figure 11: This plot shows the 'wiggling' of the small out-of-plane component α_z of the (spatially averaged) magnetization of the circular Permalloy dot; α_z comes to rest only after several ns, although the switching of the vorticity needs essentially only 42 ps, see the preceding figure. Again we have assumed $\alpha_G = 0.02$.

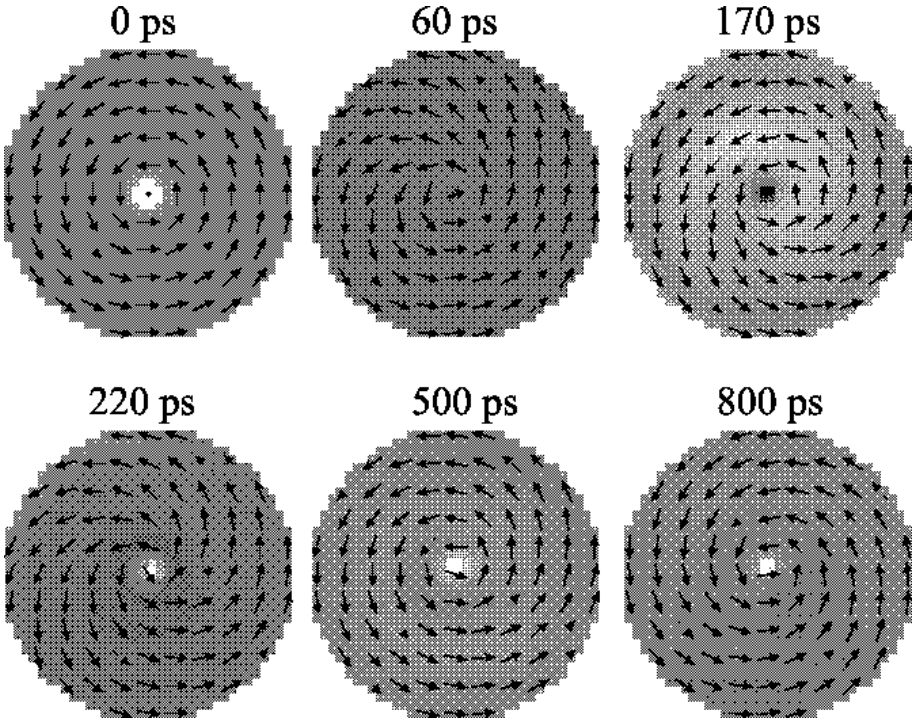

Figure 12: Here white (black) background colours mean positive (negative) values of α_z; so this 'movie sequence' shows that under the conditions described in the text the vorticity is not switched at all, whereas the central polarity changes from +1 to -1 at $t \approx 60$ ps, remains there until $t \approx 170$ ps, but returns to +1 for $t \gtrsim 220$ ps. The applied field pulses were $H_z^{\rm ext} = 1$ kOe between 0 and 60 ps, and simultaneusly $H_y^{\rm ext} = 150$ Oe between 0 and 30 ps. As before, the radius and the thickness of our Py dot were 150 and 4 nm, respectively, and the Gilbert damping was $\alpha_G = 0.02$. Note that for 60 ps and 220 ps one is no longer dealing with a vortex state, but rather with a spiral.

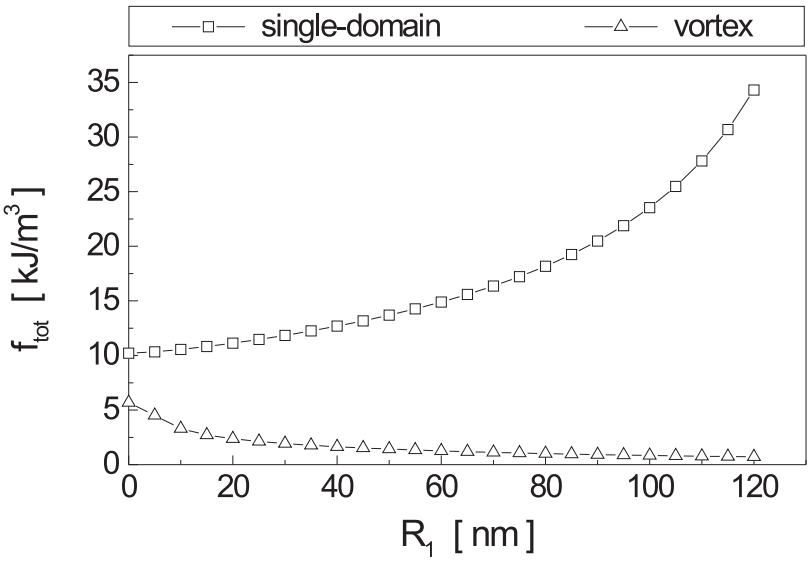

Figure 13: For flat 'nano-rings' made of Py material with fixed outer radius $R_2 = 150$ nm and thickness $t_h = 4$ nm, the total energy densities $f_{\rm tot}$ of the vortex state and the homogeneous in-plane state ('single-domain state') are presented against the inner radius R_1.

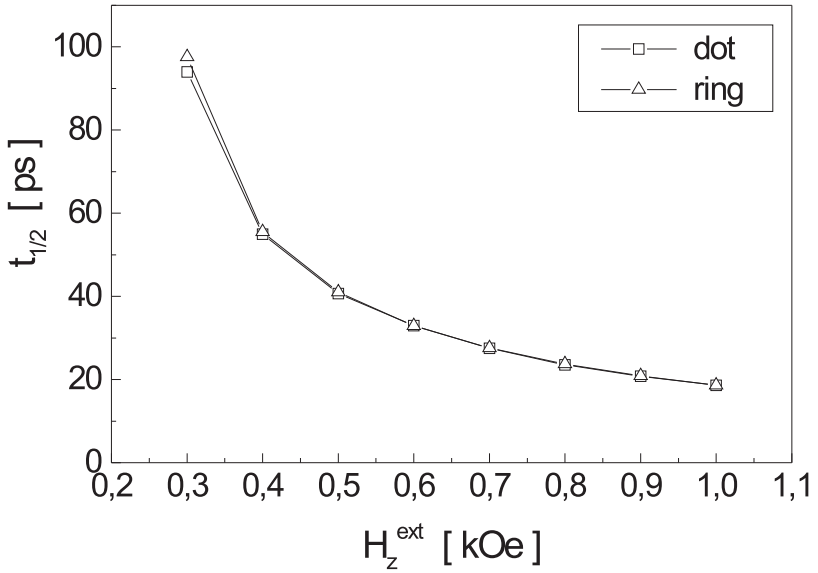

Figure 14: The switching time $t_{1/2}$ of the vorticity of a flat circular Permalloy dot (thickness $t_h = 4$ nm, radius $R = 150$ nm) and of a corresponding 'nano-ring' with outer radius $R_2 = R$ and inner radius $R_1 = R/3$ is plotted against the vertical switching field $H_z^{\rm ext}$.

Figure Captions

Fig.1a: The 'profile function' $\alpha_z(r)$ as given by our analytical ansatz is compared with results of the direct numerical simulation by the OOMMF code. Material parameters: Permalloy. The radius of the circular dot considered is 175.5 nm, the height is 6 nm.
Fig.1b: The effective radius $R_{\rm eff}$ of the vortex core is presented over the reduced thickness $T_h := \frac{t_h}{l_m}$ of the circular dot, in units of the magnetic exchange length l_m. Material parameters: Py, as in Fig. 1a.
Figure 2: The critical thickness $t_c(R)$, i.e. the line which separates the stability ranges of the vortex state from that of the in-plane single-domain state, is presented as a function of the radius R of the circular dot. Parameters of Permalloy material are used. The solid line describes our results, as given in the text; the dashed line presents the simplified approximation $t_{c,0}(R)$, also described in the text, and the circles describes the results of a numerical calculation with the OOMMF code. (Besides, the additional phase transition line separating the out-of-plane single-domain state from the in-plane single domain state would in the present plot almost coincide with the abscissa axis.)
Figure 3: The total energy density f (the solid line), and the partial energy densities of the dipolar energy (squares), exchange energy (diamonds) and Zeeman energy (triangles)) for the vortex state in a circular permalloy dot of radius $R = 150$ nm (note the vertical line) and thickness $t_h = 4$ nm are presented as a function of the shift Δ of the vortex core; for more details see the text
Figure 4: For different values of the external in-plane Zeeman field the density $f_{\rm tot}$ of the total energy of Fig. 3 is presented against the shift Δ of the vortex core. One can see that for strong enough Zeeman fields ($H_y^{\rm ext} \geq 190$ Oe) there is no longer a local minimum, i.e. the vortex vanishes ($\Delta \to \infty$), which means a transition to a single-domain state. The vertical line denotes the radius R of the circular dot.
Figure 5: For Py dots of thickness $t_h = 15$ nm and 8.3 nm, respectively, experimental results, and our theoretical results, for the in-plane annihilation fields of the vortex state are presented over the double reciprocal aspect ratio $2R/t_h$ of the dot.

Figure 6: The critical time t_c for dynamic annihilation of the vortex state by in-plane fields $H_y^{\rm ext}$ is presented against $H_y^{\rm ext}$ for different values of the Gilbert damping α_G. For further details see the text.

Figure 7: The line separating the dynamic stability and instability regions for dynamic annihilation of the vortex core by in-plane fields, as in the preceding figure, is presented in an $(\alpha_G, H_y^{\rm ext})$ plane, where α_G is Gilbert's damping parameter and $H_y^{\rm ext}$ the in-plane 'switching field'.

Figure 8: This 'movie sequence' presents the annihilation of a vortex state by an in-plane field. This is a rather slow process, which needs at least 1.5 ns, although the in-plane field is as strong as 300 Oe . Gilbert's damping parameter has been assumed to be $\alpha_G = 0.02$

Figure 9: This plot presents the typical 'switching time' $t_{1/2}$ of a vortex state by a pulsed perpendicular field $H_z^{\rm ext}$. This is a very fast process, which needs typically only ~ 40 ps, but the necessary strength of the field is very large, ~ 5000 Oe. Gilbert's damping parameter has been assumed to be $\alpha_G = 0.02$. "Theory" means the simple result $t_{1/2} = \pi/(|\gamma_0|H_z^{\rm ext})$; the other results are from OOMMF-simulations.

Figure 10: This plot shows details of the fast switching of the vorticity of our flat circular Permalloy dot of radius $R = 150$ nm and thickness $t_h = 4$ nm by a pulsed vertical field of $H_z^{\rm ext} = 5000$ Oe. The energy densities f of the dipolar energy ('stray-field') and of the exchange energy are presented over the time for the first 50 ps after the start of the perpendicular field pulse, which lasts from $t = 0$ to $t = 42$ ps.

Figure 11: This plot shows the 'wiggling' of the small out-of-plane component α_z of the (spatially averaged) magnetization of the circular Permalloy dot; α_z comes to rest only after several ns, although the switching of the vorticity needs essentially only 42 ps, see the preceding figure. Again we have assumed $\alpha_G = 0.02$.

Figure 12: Here white (black) background colours mean positive (negative) values of α_z; so this 'movie sequence' shows that under the conditions described in the text the vorticity is not switched at all, whereas the central polarity changes from +1 to -1 at $t \approx 60$ ps, remains there until $t \approx 170$ ps, but returns to +1 for $t \gtrsim 220$ ps. The applied field pulses were $H_z^{\rm ext} = 1$ kOe between 0 and 60 ps, and simultaneusly $H_y^{\rm ext} = 150$ Oe between 0 and 30 ps. As before, the radius

and the thickness of our Py dot were 150 and 4 nm, respectively, and the Gilbert damping was $\alpha_G = 0.02$. Note that for 60 ps and 220 ps one is no longer dealing with a vortex state, but rather with a spiral.

Figure 13: For flat 'nano-rings' made of Py material with fixed outer radius $R_2 = 150$ nm and thickness $t_h = 4$ nm, the total energy densities $f_{\rm tot}$ of the vortex state and the homogeneous in-plane state ('single-domain state') are presented against the inner radius R_1.

Figure 14: The switching time $t_{1/2}$ of the vorticity of a flat circular Permalloy dot (thickness $t_h = 4$ nm, radius $R = 150$ nm) and of a corresponding 'nano-ring' with outer radius $R_2 = R$ and inner radius $R_1 = R/3$ is plotted against the vertical switching field $H_z^{\rm ext}$.